ELSEVIER

Journal of Power Sources 103 (2001) 134–139

JOURNAL OF POWER SOURCES

www.elsevier.com/locate/jpowsour

The influence of target history and deposition geometry on RF magnetron sputtered $LiCoO_2$ thin films

J.F. Whitacre*, W.C. West, B.V. Ratnakumar

Jet Propulsion Laboratory, Electrochemical Technologies Group, Center for Integrated Space Microsystems, California Institute of Technology, Pasadena, CA 91109, USA

Received 3 June 2001; accepted 12 June 2001

Abstract

Thin $LiCoO_2$ films, typically used as cathode layers in thin-film solid-state batteries were RF magnetron sputter-deposited using targets that were either freshly produced, or had seen over 100 h of sputter erosion. The substrates, as received (1 0 0) silicon wafers, were either held stationary or were rocked back and forth under the target. Film texturing, grain size, composition, and thickness were examined using X-ray diffraction (synchrotron light source), inductively coupled plasma-mass spectroscopy (ICP-MS), Rutherfords backscattering spectrometry (RBS) and stylus profilometry. Films that were sputtered from the heavily used target were, on average, lithium-deficient, while films deposited using the fresh target were slightly lithium-rich. Film thickness, composition, and type of crystallographic texture varied radially, in the plane of the film in the stationary substrate case, in a pattern that reflected the sputter target erosion ring. For films deposited with substrate motion, an ovular area was defined on the film in which composition, and texturing were essentially uniform. The Li/Co ratio in the target and subsequent films was found to decrease over many hours of sputtering. Possible causes for the compositional and orientational variations observed are discussed.

Keywords: Thin $LiCoO_2$ films; Rutherfords backscattering spectrometry; RF magnetron sputtering

1. Introduction

In the past 5 years, RF magnetron sputtered metal oxide thin films, particularly, those composed of $LiCoO_2$, have emerged as a leading candidate for use as cathode layers in thin film solid-state batteries [1–3]. Films that exhibit a (1 0 4) or (1 0 1) out-of-plane crystallographic orientation (texture), have grains that are >100 nm in diameter, and display little to no lattice strain were found to be most efficient at Li intercalation and electronic conduction. It has also been shown that an annealing step, typically to 700°C, induces these desired film qualities [3]. Because this heating step is too high for many desirable substrates, such as, flexible polymer materials [4][1] or Si wafers with integrated CMOS devices [5], an effort has been undertaken in our laboratories to examine the possibility of creating $LiCoO_2$ films with the desired materials qualities without using a high temperature process step [6]. To reach this goal, a solid understanding of the deposition parameters that affect film crystallography and composition of $LiCoO_2$ when sputtered at room temperature is desired.

A range of compositions have been observed in sputtered $LiCoO_2$ films. The Li/Co ratio has been reported to be 0.88 [7] or 1.0 ± 0.1 [8] when deposited using a sputter gas consisting of 100% Ar. If sputter gases consisted of $Ar:O_2$ mixes of 1:10, 1:2, or 1:1, the Li/Co ratio was found to be 0.8 ± 0.08 [8], 0.4 [9], or 1.15 ± 0.02 [2], respectively. Concurrently, O/Co ratios were 2.7 [8], 1.92 [9], 2.2 [2]. Work completed elsewhere reports a O/Co ratio of 2.01 [10]. In all cases, the films were found to be amorphous (as per X-ray diffraction analysis) if deposited at room temperature and subsequently developed, a primarily, (0 0 3), (1 0 1), (1 1 0) or (1 0 4) out-of-plane texture upon annealing, depending on thickness [2,9]. In one case, sputtered $LiCoO_2$ films were nanocrystalline with some (0 0 3) out-of-plane texturing if sputter-deposited onto substrates held at 300°C [9].

The fact that films with such varying qualities resulted from ostensibly similar process steps led us to embark on a limited study of the relative importance of two lesser-examined deposition parameters for $LiCoO_2$ — the history of the sputter target, and the deposition geometry used.

* Corresponding author. Tel.: +1-818-354-4643.
E-mail address: whitacre@jpl.nasa.gov (J.F. Whitacre).

[1] Parylene N is one possible substrate/coating and has melting temperature of 420°C.

0378-7753/01/$ – see front matter
PII: S0378-7753(01)00849-7

2. Experimental

Three-inch lithium cobalt oxide ($LiCoO_2$) sputter targets were prepared by cold pressing (30,000 lb/in.^{2}) and sintering (900 c) $LiCoO_2$ powder purchased from Alfa Aesar. The growth chamber was a custom-designed turbo-pumped three-position RF planar magnetron sputter system configured in the sputter down geometry. A rotating substrate platen with a radius of 16 cm, and a 7 cm target to substrate distance allowed for the growth of multiple films on different substrates. The maximum chamber pressure before deposition was 3×10^{-6} Torr, though most films were grown at base pressures lower than 2×10^{-6} Torr. The $LiCoO_2$ targets were pre-sputtered for 30 min. The cathode films were sputtered in an Ar:O_2 of 3:1 with a total gas flow rate of 55 sccm and pressure of 10 mTorr. Nominal target power was 100 W, giving a power density on the sputter cathode of 2.2 W/cm^2.

During deposition, the substrate holder was either held stationary directly underneath the target or was programmed to oscillate underneath the sputter target through a range of 18° at a frequency of 0.3 Hz, a motion that rocked the substrate back and forth with an amplitude of 5 cm, as depicted in Fig. 1. The deposition rate was 190 ± 30 nm/h in the static case (see Fig. 3 for thickness profile) and was 150 ± 10 nm/h for the oscillating target case.

The films were deposited onto cleaved test-grade Si (1 0 0) wafers (with native amorphous oxide intact), and C tape. Following deposition, the films were heated to 300°C for 1 h in a dry room environment (<1% humidity). Film composition was probed using a combination of Rutherfords backscattering spectrometry (RBS) to determine O/Co ratios and inductively coupled plasma-mass spectroscopy (ICP-MS) to evaluate the Li/Co ratio. The RBS data were collected at both Caltech University and Auburn University. The Caltech pelletron system used ~1.95 MeV He ions in the "Cornell" geometry, with $\theta = 7$, $\phi = 15$, and $\tau = 0$. Beam size was roughly 0.4 cm × 0.4 cm. The RBS system at Auburn used a He ion beam with an energy of 2.03 MeV, a geometry, where $\theta = 0°$, $\phi = 10$, $\psi = 10$, and $\tau = 0$. Beam size was approximately 0.25 cm × 0.25 cm. A calibration sample consisting of a ~5 Å thick Au film on a Si wafer was used. The resulting data was modeled using the RBS data analysis software package RUMP (version 4.0). An Elan 5000 AN ICP-MS system was used to study the Li/Co ratios [11]. A comprehensive set of standards was used to minimize measurement error. The films were digested in a HNO_3:HCl (3:1) mix and subsequently diluted with a 1% HNO_3 solution before insertion into the ICP-MS system. A set of five standards containing Li/Co ratios of 0.5–1.5 was used for calibration and was run before and after data collection to verify that the ICP measurements did not drift during data acquisition. Film thicknesses were determined using an Alpha-Step 100 profilometer and cross-section SEM.

Film crystallography was examined using X-ray diffraction conducted at the Stanford Synchrotron Radiation Laboratory (SSRL), beamline 7–2 [12]. The use of a synchrotron X-ray source is justified, as these thin (typically <0.4 μm), low atomic weight films yield poor counting statistics using laboratory-based X-ray systems, particularly, when using the $\theta - 2\theta$ scattering geometry. A silicon

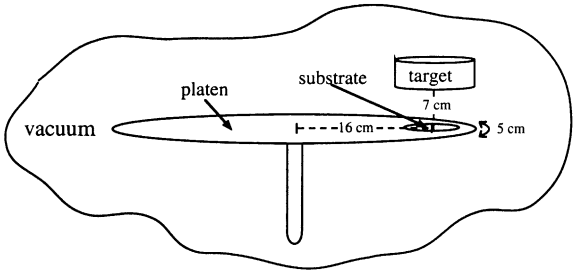

Fig. 1. Schematic representation of the deposition geometry used. The substrate rests on a platen with a 16 cm distance between the center of rotation and the center of the substrate. During sputter deposition, the substrate either rested directly under the target or was rocked back and forth with an amplitude of 5 cm.

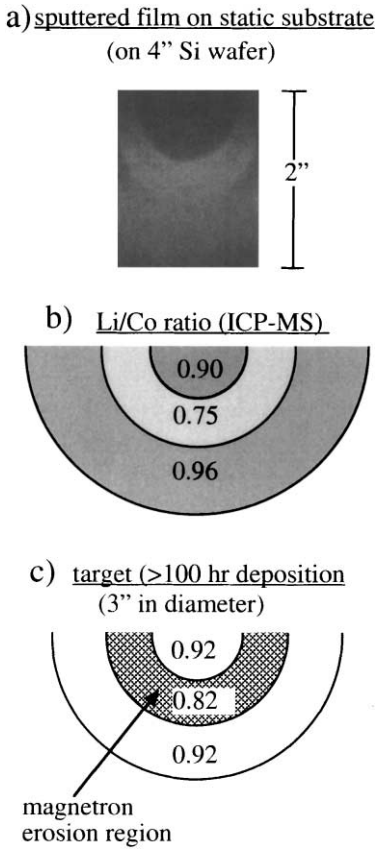

Fig. 2. (a) Image from an actual film sputtered onto a 4 in. wafer in the static geometry. Three distinct regions are evident. (b) Schematic map showing the ICP-MS determined Li/Co ratios in these regions for a film sputtered from a heavily used (>100 h) target. A similar film deposited using a fresh target has Li/Co ratios of 1.05 and 0.81 in the center and first ring (see text for uncertainty). (c) ICP-MS Li/Co ratios observed in a heavily used (>100 h) sputter target. The entire target was Li deficient, with the magnetron erosion region having the lowest Li content.

(1 1 1) monochrometer was used to select the wavelength of the X-ray beam to be 0.124 nm (10 keV), in focused mode. The films were kept in a flowing helium environment during data collection to avoid moisture contamination and minimize air scattering in the vicinity of the sample surface.

3. Results

3.1. Static deposition geometry

Fig. 2(a) and (b) shows an image and corresponding schematic of a $LiCoO_2$ film sputtered onto a 4 in. Si wafer that was held stationary during deposition using the target that had experienced over 100 h of sputtering. A pattern consisting of concentric circles is visually evident in the film, where the center was a dark brownish metallic color, encircled by a lighter metallic ring, which was in turn surrounded by another darker region. ICP-MS analysis showed that the Li/Co ratio varied on the substrate concurrent with the visual pattern: the darker inner and outer regions had Li/Co ratios of 0.90 ± 0.1, while the light intermediate ring had a lower Li/Co balance of 0.75 ± 0.07. A similar film deposited using a new sputter target had high Li/Co ratios of 1.05 ± 0.07 in the center and 0.81 ± 0.05 in the first ring. To enhance experimental statistics, over 15 measurements were made on different areas of each film.

ICP-MS analysis of the aged sputter target itself was also conducted, and the results are indicated in Fig. 2(c). All areas are Li deficient, with the lowest Li/Co ratio being in the

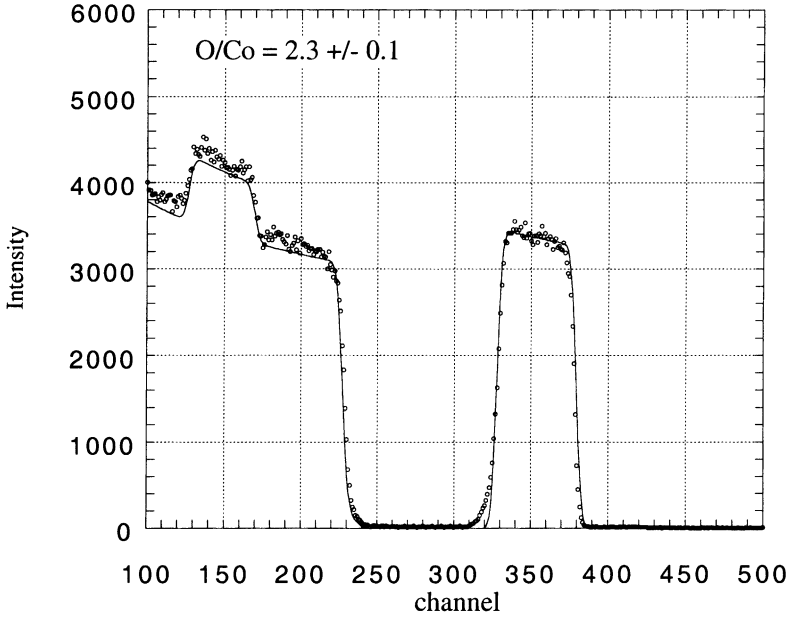

(a)

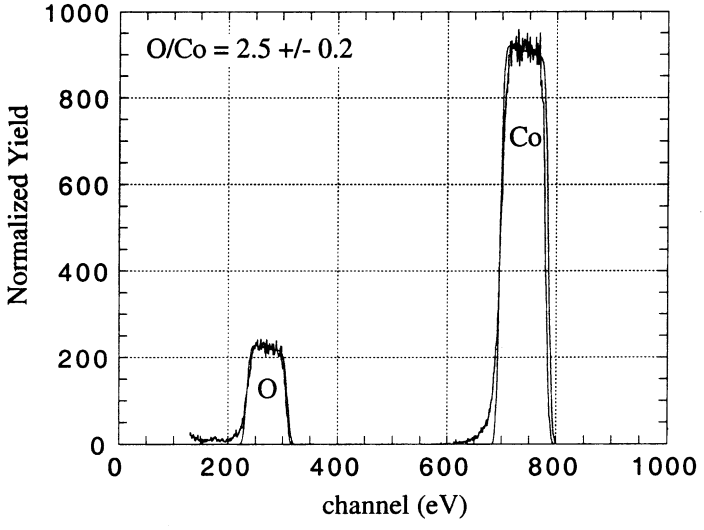

(b)

Fig. 3. RBS data from films grown (a) with a fresh target onto a C substrate, O/Co, 2.2, and (b) with a heavily used target onto a Si substrate, O/Co, 2.5.

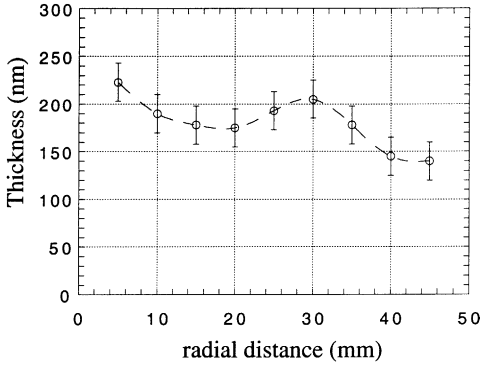

Fig. 4. Radial thickness profile of $LiCoO_2$ sputtered in Ar using a stationary substrate holder. This data was collected using an Alpha Step 100 stylus profilometer.

magnetron erosion region. In particular, the Li/Co ratio was 0.82 ± 0.05 in the wear ring and the center or outer areas had a Li/Co ratio of 0.92 ± 0.05.

Fig. 3(a) and (b) shows an example of the RBS data collected for these films. Computer simulation using the computer program, RUMP (version 4.0, Computer Graphics Systems, Cornell University) showed that O/Co ratio was in the range of 2.5 ± 0.2 in all areas of the films sputtered from the used target and was 2.2 ± 0.3, in the films sputtered from the fresh target. The uncertainties in these values are a combined result of point-to-point variation in the film as well as the error generated when modeling the data.

Film thickness is plotted as a function of radial distance from the center of the substrate in Fig. 4. This film was deposited for 1 h. The thickness varies in a pattern roughly corresponding to the visual and compositional patterns described above. The values range from roughly 150–225 nm, with the two maxima occurring at the center of the substrate and at the outer edge of the first ring.

X-ray diffraction results show that the crystallites in the film can display different crystallographic orientational differences depending on substrate location. Diffraction data from a ~280 nm thick $LiCoO_2$ film are shown in Fig. 5. The pattern collected from the central area shows a strong (1 0 4) peak and relatively weak (1 0 1) and (0 0 3) peaks, which is consistent with a film that has a strong (1 0 4) out-of-plane texture. The middle band area had a weaker (1 0 4) peak and some (1 0 1) scattering, whereas the outermost area showed a predominantly (0 0 3) texture. The average grain size, as calculated from peak broadening using the Scherrer formula was at least 8 nm.[2] The films grown from a fresh target under similar conditions displayed the same types of textures at the same locations despite the significant differences in film composition. In films deposited using fresh and used targets, grain size and film crystallography were nominally the same.

[2] Because, so few diffraction peaks were evident, the microstrain effects that also cause peak broadening could not be ruled out, though a minimum grain size can be established.

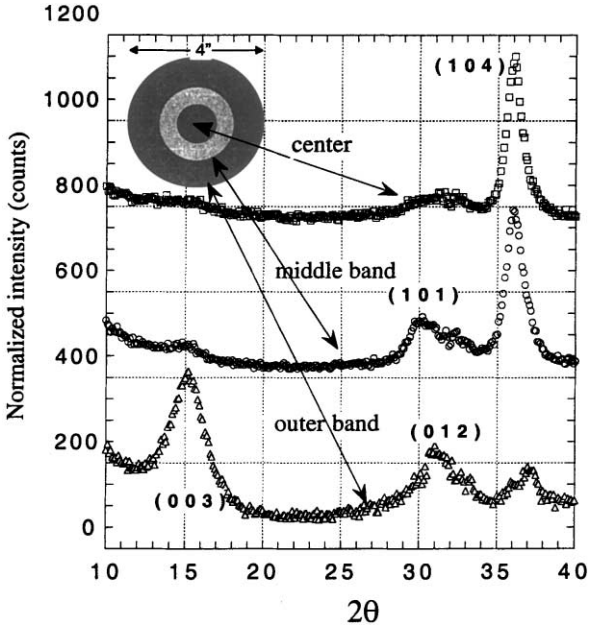

Fig. 5. X-ray diffraction patterns collected from a $LiCoO_2$ film sputtered in Ar onto a stationary substrate from a target that had seen >100 h of use. Though the diffraction patterns collected from different regions of the film are consistent with those expected from $LiCoO_2$, different types of out-of-plane texture are observed.

3.2. Films deposited with substrate motion

It is desirable to have the ability to sputter-deposit a film that is uniform in composition and thickness over a large portion of the substrate. To this end, the substrate was rocked under the sputter target during deposition as described in Section 2. The result was a film with a large, light metallic ovular area (as shown in Fig. 5). This area had major and minor axes that were 7 and 5 cm, respectively and had nominally the same thickness everywhere. Fig. 5 shows the composition and diffraction results for a film grown using this geometry with a newly fabricated $LiCoO_2$ target that had seen less than 10 h of sputtering. The inset figure is an image of a 4 in. Si wafer substrate that illustrates the location and shape ovular area. ICP-MS and RBS analysis indicated that the Li/Co ratio in the ovular substrate region was 1.1 ± 0.1 while the O/Co ratio was 2.2 ± 0.1. The diffraction data show that there was a strong (1 0 4) peak observed in the ovular area, which is consistent with the existence of a strong (1 0 4) out-of-plane texture. Outside the center oval, the relative intensity of the (1 0 1) to (1 0 4) peak was larger, consistent with a mixed (1 0 1) and (1 0 4) texture. The average grain size, as calculated from peak broadening using the Scherrer formula, was at least 8 nm [13].

3.3. Summary of results

Table 1 contains a summary of the analytical results described above. The film composition range and the type

Table 1
Chart showing the composition and type of texture in RF magnetron sputtered $LiCoO_2$ thin films for different target histories and deposition geometries

Target age (h used)	Geometry	Composition[a]	Type of texture
Fresh (<10)	Motion	$Li_{1.1}CoO_{2.2}$ in oval	(1 0 4) in oval
	Motion	$Li_{1.05}CoO_{2.2}$ in center	(1 0 4) in center
	Static	$Li_{0.81}CoO_{2.2}$ First ring	(1 0 1)/(1 0 4) first ring
Heavy use (>100)	Motion	$Li_{0.9}CoO_{2.5}$ in oval	(1 0 4) in oval
	Static	$Li_{0.9}CoO_{2.5}$ in center	(1 0 4) in center
	Static	$L_{0.75}CoO_{2.5}$ in first ring	(1 0 1)/(1 0 4) mix first ring
	Static	$Li_{0.9}CoO_{2.5}$ second ring	(0 0 3) in outer ring

[a] See text for uncertainty.

of texture are described as a function of target history and deposition geometry.

4. Discussion

$LiCoO_2$ films deposited using a stationary substrate holder possessed significant lateral variation in composition, thickness, and type of out-of-plane texture. The pattern of these compositional variations corresponded to similar variations in the sputter target itself, where there was a lower Li/Co ratio in the magnetron erosion ring area. The relationship between variations in target composition and subsequent film composition has been investigated previously for sputtered metallic films: in the case of a target with a ''bull's eye'' pattern of different materials, there was a distinct lateral compositional in the film that corresponded to the distribution of material in the target [13]. The degree to which this effect manifests itself depends upon the mean free path of the average sputtered neutral adatom compared to the target-to-substrate distance. In our case, with a sputter pressure of 10 mTorr, the sputtered neutral mean free path is ~2.7 cm. With a target-to-substrate distance of 7 cm, it is likely that the neutrals have, on average, only 2–4 collisions before reaching the growth surface. So, few collisions are not enough to fully thermalize or randomize the adatom flux.

Films grown using sputter targets that had seen many hours of sputtering were shown to have a lower Li/Co ratio. This result was then related to target composition. The cause of the Li deficiency in the aged targets is not well understood. Li is thought to have a lower sputter yield than Co or O [14], making outright preferential sputtering of Li, unlikely. The formation and surface diffusion (away from the magnetron erosion ring) of Li_2O on lithium compound sputter targets has been documented for the Li_4SiO_4 system [15,16]. It has also been established that oxides formed on compound sputter targets have different sputter yields than the constituents from which they were formed [17,18]. One possible scenario consistent with the results would occur if Li_2O is created continually at the target surface (with some Li diffusing from beneath the surface) and is then preferentially sputtered over Co or CoO_2. If this were to be so, an excess of Li in films grown from freshly made targets is expected. Indeed, the data from such films, as shown in Fig. 4, indicates that the Li/Co ratio was 1.1 ± 0.1. Further, the area of greatest Li depletion should be where the majority of the sputtering events occur in the magnetron erosion ring. The data also show that this is the case. The O/Co ratios also vary depending on the target age. It is likely that this effect is also linked to the loss of Li over time. A complete set of experiments is necessary, however, before a conclusive statement concerning the nature of this phenomenon can be made.

The results also show that both the grain size and type of texture are not strongly dependent upon target history and subsequent film composition. As can be seen in Table 1, the nominal out-of-plane texture is the same for the films regardless of the sputter target history. The variations in texture are more correlated to the deposition geometry, where the films sputtered onto wafer had textures ranging from (1 0 4) to (0 0 3) depending on what location on the substrate the data was collected from and what deposition geometry was used. The mechanisms that determine film texture are insensitive to composition, yet sensitive to the substrate–target geometry, a parameter that is most closely linked to local substrate heating along with incident adatom kinetic energy and directionality. This finding is consistent with those theories that attribute film texturing to mechanisms such as surface energy minimization [19], residual stress [20], or preferential sputtering [21].

5. Summary

This study has shown that composition and texture in RF planar magnetron sputtered $LiCoO_2$ thin film cathodes critically depends on the deposition geometry used as well as the use history of the sputter target. In particular, it was shown that a $LiCoO_2$ target becomes Li deficient over time, and that this deficiency is greatest in the magnetron erosion region. This compositional gradient is subsequently reflected in the sputtered films, where a distinct visual and compositional pattern is evident if the substrate is held stationary under the target during growth. The type of out-of-plane texture in the films was found to depend on the deposition geometry used, and to be independent of the

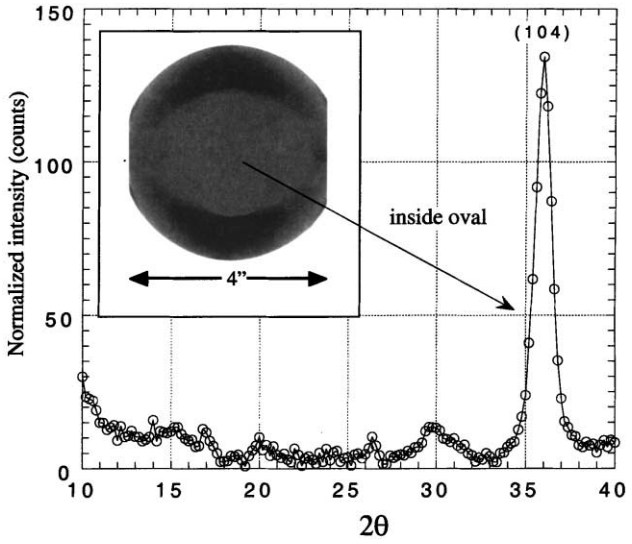

Fig. 6. Inset shows a partial image of a 4 in. Si substrate with ~200 nm of $LiCoO_2$ deposited onto it at room temperature using a fresh target and the rocking substrate motion. The lighter ovular area is ~5 cm × 7 cm in size and is uniform in thickness and composition as indicated. The diffraction pattern is from the ovular area and shows that in this region there was a strong degree of (1 0 4) out-of-plane texture.

sputter target history. Films sputtered using a rocking substrate motion were found to have an ovular area that had a uniform Li/Co composition and a desirable (1 0 4) out-of-plane texture. These films have been incorporated into thin film solid state batteries that have capacities that approach the theoretical limits of the $LiCoO_2$ system when discharged at a suitably low current [6] (Fig. 6).

Acknowledgements

This work was carried out at the Jet Propulsion Laboratory, California Institute of Technology, under contract with the National Aeronautics and Space Administration. The authors acknowledge the financial support of the Center for Integrated Space Microsystems at JPL. Additional funding was provided through the 1-year Cross Enterprise Technology Development Program (CETDP) JUPN 632. The X-ray diffraction work was conducted at SSRL, a DOE facility. A portion of the RBS data was collected at Auburn University, facilities supervised by Professor John Williams.

References

[1] J.B. Bates, G.R. Gruzalski, N.J. Dudney, C.F. Luck, Xiaohua Yu, Solid State Ionics 70 (1994) 619–628.
[2] B. Wang, J.B. Bates, F.X. Hart, B.C. Sales, R.A. Zuhr, J.D. Robertson, J. Electrochem. Soc. 143 (10) (1996) 3203.
[3] F.X. Hart, J.B. Bates, J. Appl. Phys. 81 (12) (1998) 7560.
[4] Parylene Conformal Coatings Specifications and Properties, Specialty Coatings Systems Inc., 2000.
[5] R.C. Jaeger, Introduction to Microelectronic Fabrication, Addison–Wesley, Reading, MA, 1993.
[6] J.F. Whitacre, W.C. West, E. Brandon, R.V. Bugga, S. Surampudi, in: Proceedings of the Electrochemical Society, Phoenix, AZ, October 2000, in press.
[7] P. Fragnaud, T. Brousse, D.M. Schleich, J. Power Sources 63 (1996) 187–191.
[8] H. Benqlilou-Moudden, G. Blondiaux, P. Vinatier, A. Levasseur, Thin Solid Films 333 (1998) 16–19.
[9] G. Wei, T.E. Haas, R.B. Goldner, Solid State Ionics 58 (1992) 115–122.
[10] E.J. Bouwman, B.A. Boukamp, H.J.M. Bouwmeester, H.J. Wondergem, P.H.L. Notten, J. Electrochem. Soc. 148 (4) (2001) A311–A317.
[11] L.R. Doolittle, Nuclear Instrumental Methods, B9 344, 1985.
[12] S.G. Malhotra, Z.U. Rek, S.M. Yalisove, J.C. Bilello, Analysis of thin film stress measurement techniques, Thin Solid Films 301 (1997) 45.
[13] G.C. Swartz, R.E. Jones, L.I. Maissel, J. Vac. Sci. Technol. 6 (1969) 351.
[14] Maissel and Glang, Handbook of Thin Film Technology, McGraw-Hill, New York, 1970.
[15] N.J. Dudney, J.B. Bates, J.D. Robertson, J. Vac. Sci. Techol. A 11 (2) (1993) 377–389.
[16] N.J. Dudney, J.B. Bates, R.A. Zuhr, C.F. Luck, J.D. Robertson, Solid State Ionics 53/56 (1992) 655–661.
[17] E.H. Hasseltine, F.C. Hurlbut, N.T. Olson, H.P. Smith, J. Appl. Phys. 38 (1967) 4313.
[18] E. Hollands, D.S. Campbell, J. Mater. Sci. 3 (1968) 544.
[19] D.B. Knorr, Materials Science Forum 157/162 (1994) 1327–1336.
[20] J.B. Bates, N.J. Dudney, B.J. Neudecker, F.X. Hart, H.P. Jun, S.A. Hackney, J. Electrochem. Soc. 147 (1) (2000) 59–70.
[21] L. Dong, D.J. Srolovitz, J. Appl. Phys. 84 (9) (1998) 5261–5269.